



Pharmaceutical Nanotechnology

Anti-tumor activity of all-trans retinoic acid-incorporated glycol chitosan nanoparticles against HuCC-T1 human cholangiocarcinoma cells

Kyu-Don Chung^a, Young-Il Jeong^{b, **}, Chung-Wook Chung^b, Do Hyung Kim^b, Dae Hwan Kang^{b,*}^a Department of Anesthesiology and Pain Medicine, College of Medicine, The Catholic University, Seoul 137-701, Republic of Korea^b National Research and Development Center for Hepatobiliary Disease, Pusan National University Yangsan Hospital, Gyeongnam 626-770, Republic of Korea

ARTICLE INFO

Article history:

Received 7 September 2011

Received in revised form 26 October 2011

Accepted 31 October 2011

Available online 9 November 2011

Keywords:

All-trans retinoic acid

Glycol chitosan

Nanoparticles

Cholangiocarcinoma

Invasion

ABSTRACT

The aim of this study is to investigate antitumor activity of all-trans retinoic acid (RA)-incorporated glycol chitosan (GC) nanoparticles. RA-incorporated GC nanoparticles were prepared by electrostatic interaction between RA and amine group of GC. RA-incorporated GC nanoparticles have spherical shape and their particle size was 317 ± 34.5 nm. They were simply reconstituted into aqueous solution without changes of intrinsic properties. RA-incorporated GC nanoparticles were evidently inhibited the proliferation of HuCC-T1 cholangiocarcinoma cells at higher than 20 $\mu\text{g}/\text{ml}$ of RA concentration while empty GC vesicles did not affect to the viability of tumor cells. Apoptosis and necrosis analysis of tumor cells with treatment of RA or RA-incorporated GC nanoparticles also supported these results. Invasion test using Matrigel® also showed that invasion of tumor cells was significantly inhibited at higher than 20 $\mu\text{g}/\text{ml}$ of RA concentration. Wound healing assay also showed that RA-incorporated GC nanoparticles were inhibited migration of tumor cells as similar to RA itself. Our results suggested that RA-incorporated GC nanoparticles is a promising vehicles for RA delivery to HuCC-T1 cholangiocarcinoma cells.

© 2011 Elsevier B.V. All rights reserved.

1. Introduction

Cholangiocarcinoma (CC) is one of the most aggressive cancers arising from biliary tract epithelia, and its global incidence has recently been shown to be increasing (Lim, 2003; Reddy and Patel, 2006; Sandhu and Roberts, 2008; Singh and Patel, 2006). CC is characterized by poor prognosis and difficulties in diagnosis (Reddy and Patel, 2006; Sandhu and Roberts, 2008). Curative treatment options for CC are practically lacking and the median survival of advanced CC patients is <24 months (Sandhu and Roberts, 2008; Welzel et al., 2006). Even though one unique option for curative treatment of CC may be surgical resection, most of the diagnosed patients are frequently identified at an advanced stage of CC, which is not amenable to surgery. Therefore, palliative therapies, including endoscopic stent placement, chemotherapy, radiation therapy, and photodynamic therapy (PDT) are regarded as feasible treatment options to lengthen patient survival time. Furthermore, CC is known to be resistant to traditional chemotherapy and

radiotherapy (Blehacz and Gores, 2008; Sirica, 2005). The progression of CC is not only dependent on proliferation of the tumor but also on invasion, metastasis, and spreading (Bhuiya et al., 1992; Rosai, 1996). Because most chemotherapeutic options concentrate on inhibiting cell proliferation, a more effective treatment option is required for the physiological considerations of CC.

The retinoids and related compounds such as all-trans retinoic acid (RA) are known to regulate cell behaviour and to play key roles in determination of cell fate (Morris-Kay, 1992; Noll and Miller, 1994). Especially, RA is effective for the treatment of epithelial and hematological malignancies such as breast cancer (Kalmekerian et al., 1994), head and neck cancer (Giannini et al., 1997), ovarian adenocarcinoma (Krupitza et al., 1995), human malignant gliomas (Defer et al., 1997), and acute promyelocytic leukemia (APL) (Huang et al., 1988). However, the clinical application of RA is limited due to its side effects such as acute retinoid resistance, hypertriglyceridemia, mucocutaneous dryness, headache, and cancer relapse after a brief remission (Mundi et al., 1992), (Conley et al., 1997; Frankel et al., 1992). Furthermore, drawbacks of RA such as photosensitivity, local irritating reactions, and poor aqueous solubility (0.1 μM at pH 7.3) were reported (Lehman et al., 1988; Szuts and Harosi, 1991). These drawbacks of RA have led to development of various formulations of RA such as RA-loaded microspheres (Choi et al., 2001; Giordano et al., 1993), liposomes (Estey et al., 1999), solid lipid nanoparticles (Lim and Kim, 2002), and polymeric micelles (Jeong et al., 2006). Especially, positively charged polymers, i.e. nanoparticles based on ion-complex

* Corresponding author at: National Research & Development Center for Hepatobiliary Cancer, Pusan National University YangSan Hospital, Beomeo-ri, Mugeum-eup, Yangsan, Gyeongnam 626-770 Republic of Korea.

Tel.: +82 55 360 3870; fax: +82 55 360 3879.

** Corresponding author. Tel.: +82 55 360 3873; fax: +82 55 360 3879.

E-mail addresses: nanomed@naver.com (Y.-I. Jeong), sulsulpul@yahoo.co.kr (D.H. Kang).

formation between RA and polymers, are feasible carriers for RA because RA is an acidic compound. Thünemann et al. (Thünemann and Beyermann, 2000; Thünemann et al., 2000) reported the formation of RA-incorporated nanoparticle complexes with positively charged macromolecules such as polyethyleneimine (PEI) and poly(ethylene oxide)-b-poly(L-lysine).

The aim of this study was to test the antitumor activity of RA or RA-incorporated GC nanoparticles against HuCC-T1 human CC cells. Furthermore, retinoids are known to have anti-proliferation, anti-migration, and anti-invasive activity against human malignant gliomas (Bouterfa et al., 2000; Rotan, 1991), suggesting that retinoids are suitable anticancer agents to inhibit progression of tumors. Antitumor activity of RA or RA-incorporated nanoparticles were rarely investigated against cholangiocarcinoma. Therefore, we investigated the anti-proliferation, anti-migration, and anti-invasion effects of RA and RA-incorporated nanoparticles on HuCC-T1 human CC cells.

2. Materials and methods

2.1. Materials

GC, RA, dimethylformamide (DMF), and dialysis membranes (MWCO = 12,000 g/mol) were purchased from Sigma Chem. Co. Ltd. (St. Louis, MO, USA). Dimethylsulfoxide (DMSO) was purchased from Sigma Chem. Co. Ltd. as a cell culture grade.

2.2. Preparation of RA-incorporated GC nanoparticles

RA-incorporated GC nanoparticles were prepared as previously reported (Jeong et al., 2006). Briefly, 5 mg of RA was dissolved in 1 mL of DMF, and 40 mg of GC was dissolved in 10 mL of deionized water. RA/DMF solution (1 mL) was slowly dropped into aqueous GC solution for 10 min and additionally stirred for 20 min under darkened conditions. Then, solvent was removed by dialysis against deionized water for 1 day using a dialysis membrane (MWCO = 12,000 g/mol). The dialyzed solution was lyophilized and analyzed.

To measure drug contents and loading efficiency, the volume of the dialyzed solution was adjusted to 20 mL by adding deionized water, and then 100 μ L of this solution was diluted with 9.9 mL of DMSO. Empty GC vehicles were prepared similar to RA-incorporated GC nanoparticles, but in the absence of RA. Empty vehicles of GC were used as a blank test. The drug contents were measured using a UV spectrophotometer (UV-1200, Shimadzu Co. Ltd., Kyoto, Japan) at 365 nm. Drug contents = [amount of RA in the nanoparticles/weight of nanoparticles] \times 100. Loading efficiency = [residual amount of RA in the nanoparticles/feeding amount of RA] \times 100.

2.3. Characterization of RA-incorporated GC nanoparticles

The morphology of RA-incorporated GC nanoparticles was observed using a field emission scanning electron microscope (FE-SEM, Hitachi-S4700). One drop of RA-incorporated GC nanoparticle solution was placed onto a cover glass and dried at room temperature. Nanoparticles were coated with gold using an ion coater and observed at 20 kV.

Particle size was analyzed by Nano-ZS (Malvern, Worcestershire, UK). A sample solution prepared via the dialysis method was used to determine particle size (concentration: 0.1 wt%).

2.4. Cell culture

Human CC cells (HuCC-T1) were purchased from the Health Science Research Resources Bank (Osaka, Japan). Cells were

maintained in RPMI 1640 medium supplemented with 10% fetal bovine serum at 37 °C in a humidified atmosphere with 5% CO₂.

2.5. Proliferation inhibition assay

Growth inhibition was determined by the MTT assay. Aliquots containing 3×10^3 cells were seeded into each well of a 96-well plate and incubated overnight in a 5% CO₂ incubator at 37 °C. Then, RA dissolved in DMSO was diluted with RIMI 1640 (10% FBS) and added to each well. RA-incorporated GC nanoparticles prepared as described above were filtered using a 0.8 μ m syringe filter, diluted with RIMI 1640 (10% FBS), and used to treat the tumor cells. Treatment with RIMI 1640 (10% FBS) with 0.1% (v/v) DMSO was used for a control. The cells were incubated for an additional 24 h or 48 h at 37 °C in a 5% CO₂ incubator. Subsequently, 25 μ L of MTT (3 mg/mL in PBS) was added to each well, and cells were incubated for an additional 4 h. Then, 100 μ L of SDS-HCl solution (SDS 10% w/v, 0.01 M HCl) was added to each well and incubated for an additional 12 h in 37 °C, in a 5% CO₂ incubator. The absorbance was then measured at a wavelength of 570 nm using an Infinite M200 pro reader (Tecan Austria GmbH, Salzburg, Austria). All experiments were conducted in triplicate. The viable cells were expressed as a percent of control. Results are calculated as the mean \pm SD of 3 different experiments.

2.6. Cytotoxicity assay

To determine cytotoxicity test against tumor cells, 3×10^4 cells per well were seeded in 96-well plate and incubated overnight in a 5% CO₂ incubator at 37 °C. Then, the medium was exchanged with fresh serum-free medium and incubated 12 h in a 5% CO₂ incubator at 37 °C. RA dissolved in DMSO was diluted with fresh serum-free medium and added to each well. RA-incorporated GC nanoparticles were also diluted with fresh serum-free medium used to treat tumor cells. Serum-free RIMI 1640 with 0.1% (v/v) DMSO was used as a control treatment. The cells were incubated for an additional 24 h–72 h at 37 °C in a 5% CO₂ incubator. Subsequently, 25 μ L of MTT (3 mg/mL in PBS) was added to each well, and cells were incubated for an additional 4 h. Then, 100 μ L of SDS-HCl solution (SDS 10% w/v, 0.01 M HCl) was added to each well and incubated for an additional 12 h at 37 °C, in a 5% CO₂ incubator. The absorbance was then measured at a wavelength of 570 nm using an Infinite M200 pro reader (Tecan, Switzerland). All experiments were conducted in triplicate. The viable cells were expressed as a percent of control. Results are calculated as the mean \pm SD of 3 different experiments.

2.7. Flow cytometric analysis

Flow cytometric analysis was performed as previously described (Kim et al., 2011). Two propidium iodide reagents (P4170, Sigma) and FITC-annexin V (sc-4252 FITC, Santa Cruz, CA, 95060, USA) were used to identify apoptosis and necrosis of HuCC-T1 cells, respectively. Cells were treated with various concentrations of RA or RA-incorporated GC nanoparticles for 24 h. Then, the cells were collected and washed with PBS. The collected pellets were resuspended with binding buffer (10 mM HEPES pH 7.4, 150 mM NaCl, 5 mM KCl, 1 mM MgCl₂, and 1.8 mM CaCl₂) containing FITC-annexin V (1 μ g/mL) and further incubated for 30 min. Ten minutes prior to termination of incubation, PI (10 μ g/mL) was added to the cells to stain necrotic cells under dark conditions. Then, the cells were immediately analyzed with a FACScan flow cytometer (Becton Dickinson Biosciences, San Jose, CA, USA) equipped with an excitation laser line at 488 nm. The PI was collected through a 575 \pm 15 nm band pass filter.

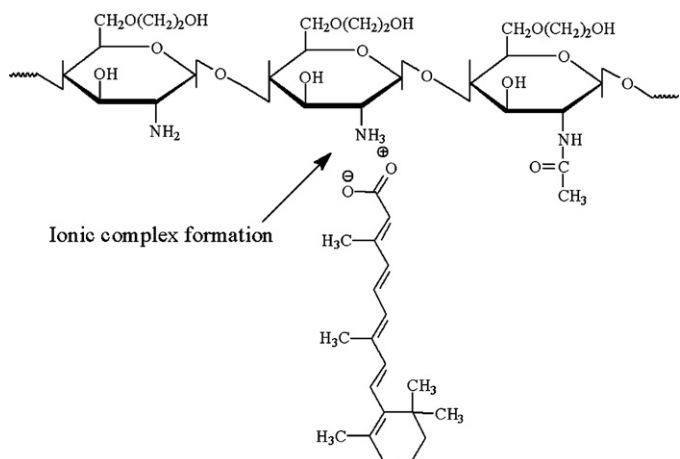


Fig. 1. Schematic illustration of RA-incorporated GC nanoparticles based on ion-complex formation.

2.8. Matriigel assay

The invasion assay was performed using a transwell chamber as previously reported (Jin et al., 2009). Polyethylene terephthalate membranes (PET membrane, pore size: 8 μm) (BD Falcon, Franklin Lakes, NJ, USA) were coated with Matriigel® (Becton Dickinson, Bedford, MA, USA) diluted in serum-free RPMI 1640 medium (RPMI:ECM = 4:1) at 4 °C. HuCCT-1 cells were seeded at a density of 2×10^4 cells in 100 μL of serum-free media in the upper compartment of a transwell chamber, and allowed to invade the PET membrane and enter the lower chamber for 2 days. The lower chamber was filled with RPMI medium supplemented with 10% FBS. Various concentrations of RA, RA-incorporated GC nanoparticles, or empty GC vehicles were added to the lower chamber. Then, non-invaded cells on the upper surface of the membrane were removed, and the invaded cells on the lower surface of the membrane were stained with a Hemacolor® Rapid staining Kit (Merck, Darmstadt, Germany). The invading cells were observed with an optical microscope (Micros Austria, Veit/Glan, Austria) and the number of cells in 4 randomly selected microscopic fields per membrane was counted.

2.9. Wound healing assay

A wound healing assay of HuCC-T1 CC cells was performed using a wound healing assay kit containing ibidi Culture-Inserts (ibidi GmbH, Germany). Aliquots containing 5×10^5 cells in RPMI 1640 (supplemented with 10% FBS) media were seeded on 6 well plates and cells were exposed to RA or RA-incorporated GC nanoparticles (1 or 5 $\mu\text{g}/\text{mL}$ of RA) at 37 °C and 5% CO₂ for 24 h. After 24 h, the cells were washed twice with PBS and harvested by trypsinization. Then, 5×10^4 cells in serum free RPMI1640 were seeded into culture inserts following incubation for 24 h. The zone of wound healing and migrated cells was observed using light microscopy. For migration of tumor cells, serum-free medium was used to avoid proliferation-dependent migration of tumor cells.

3. Results

3.1. Characteristic of RA-incorporated GC nanoparticles

RA-incorporated nanoparticles were prepared by mixing of a GC aqueous solution and a RA organic solution. Nanoparticles were created via formation of an ion complex between the acid group of RA and the amine group of GC, as shown in Fig. 1. To confirm

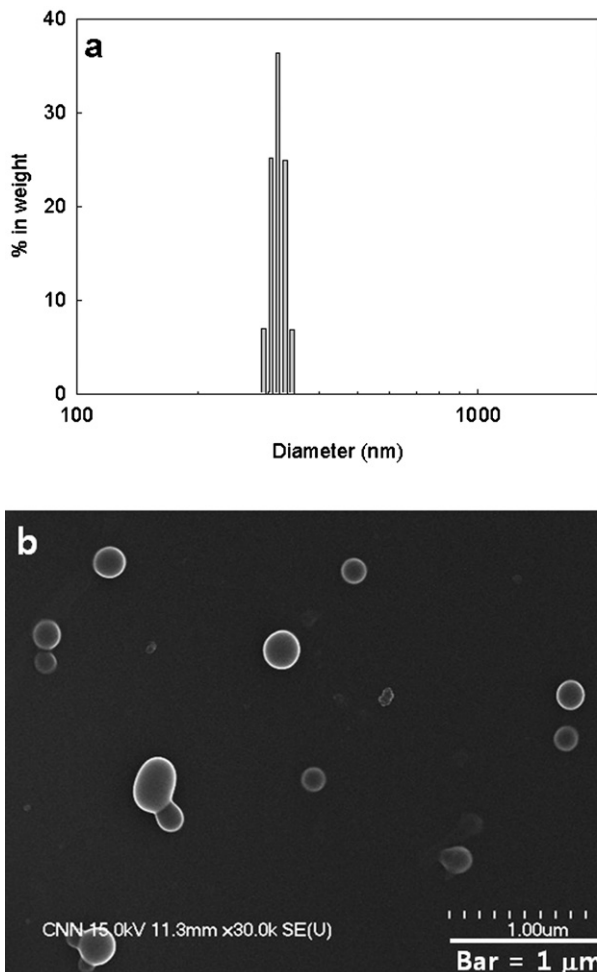


Fig. 2. Typical particle size distribution (a) and FE-SEM image (b) of RA-incorporated GC nanoparticles. (a) Weight average particle size: 317 ± 34.5 nm. (b) Bar = 1 μm .

nanoparticle formation, particle size was measured and morphology was observed using FE-SEM. As shown in Fig. 2(a), the particle size of the RA-incorporated GC nanoparticles was 317 ± 34.5 nm, and they displayed a narrow size distribution. Their morphology was a spherical shape with a 200–400 nm particle size. Even though some aggregated particles with a bigger size were found, the size of most nanoparticles was similar to the particle size measurement. Empty nanoparticles were prepared in a manner similar to preparation of drug-loaded particles (data not shown). However, particle size could not be measured and no nano-sized particles were found by FE-SEM observation. These results indicated that GC nanoparticles were only created via ion complex formation between RA and GC. Drug contents and loading efficiency were ~9.5% (w/w) and 84% (w/w), respectively.

3.2. Cell cytotoxicity of RA-incorporated GC nanoparticles

HuCC-T1 CC cells were used to study the antitumor activity of RA-incorporated GC nanoparticles against cholangiocarcinoma cells. The antitumor activity of RA-incorporated GC nanoparticles was tested using a proliferation inhibition assay and cytotoxicity assay. For the proliferation inhibition assay, a small number of cells were seeded and exposed to RA or RA-incorporated GC nanoparticles. As shown in Fig. 3(a)–(c), proliferation of tumor cells was inhibited according to the increase of RA concentration and time course. RA itself had a small inhibitory effect on the proliferation of tumor cells until reaching a concentration of 20 $\mu\text{g}/\text{mL}$ for 2

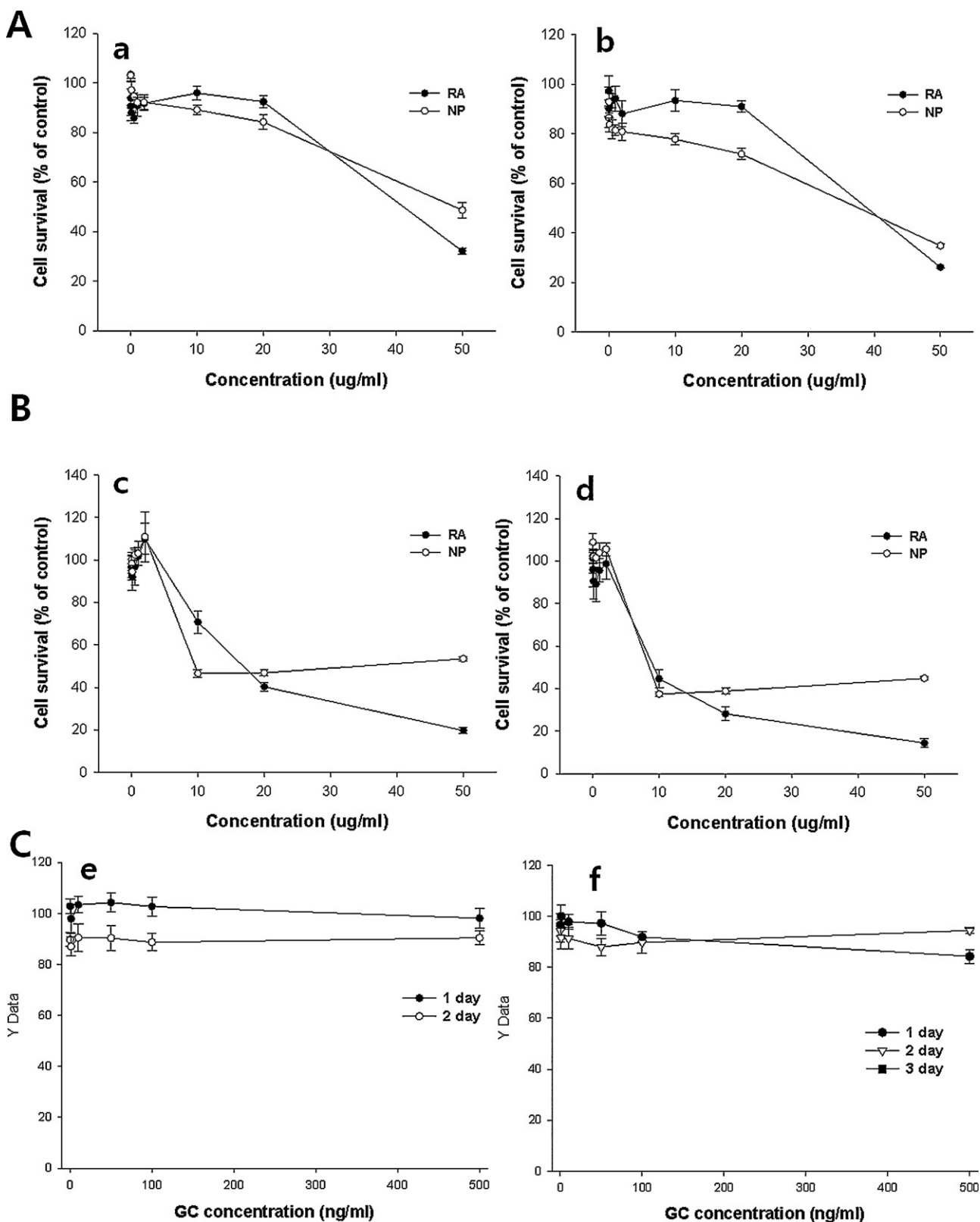


Fig. 3. Growth inhibitory effect (A) and cytotoxicity (B) of RA or RA-incorporated GC nanoparticles against HuCC-T1 human CC cells. For growth inhibition test, 3×10^3 tumor cells per well were seeded in 96 well plate and cells were exposed to RA or RA-incorporated GC nanoparticles for 1 day (a) and 2 day (b). For cytotoxicity test, 3×10^4 tumor cells per well were seeded in 96 well plate and cells were exposed to RA or RA-incorporated GC nanoparticles for 1 day (c) and 2 day. Growth inhibitory effect (e) and cytotoxicity (f) of empty GC nanoparticles (C). RPMI1640 supplemented with 10% FBS were used for growth inhibition test and serum-free RPMI1640 were used for cytotoxicity test.

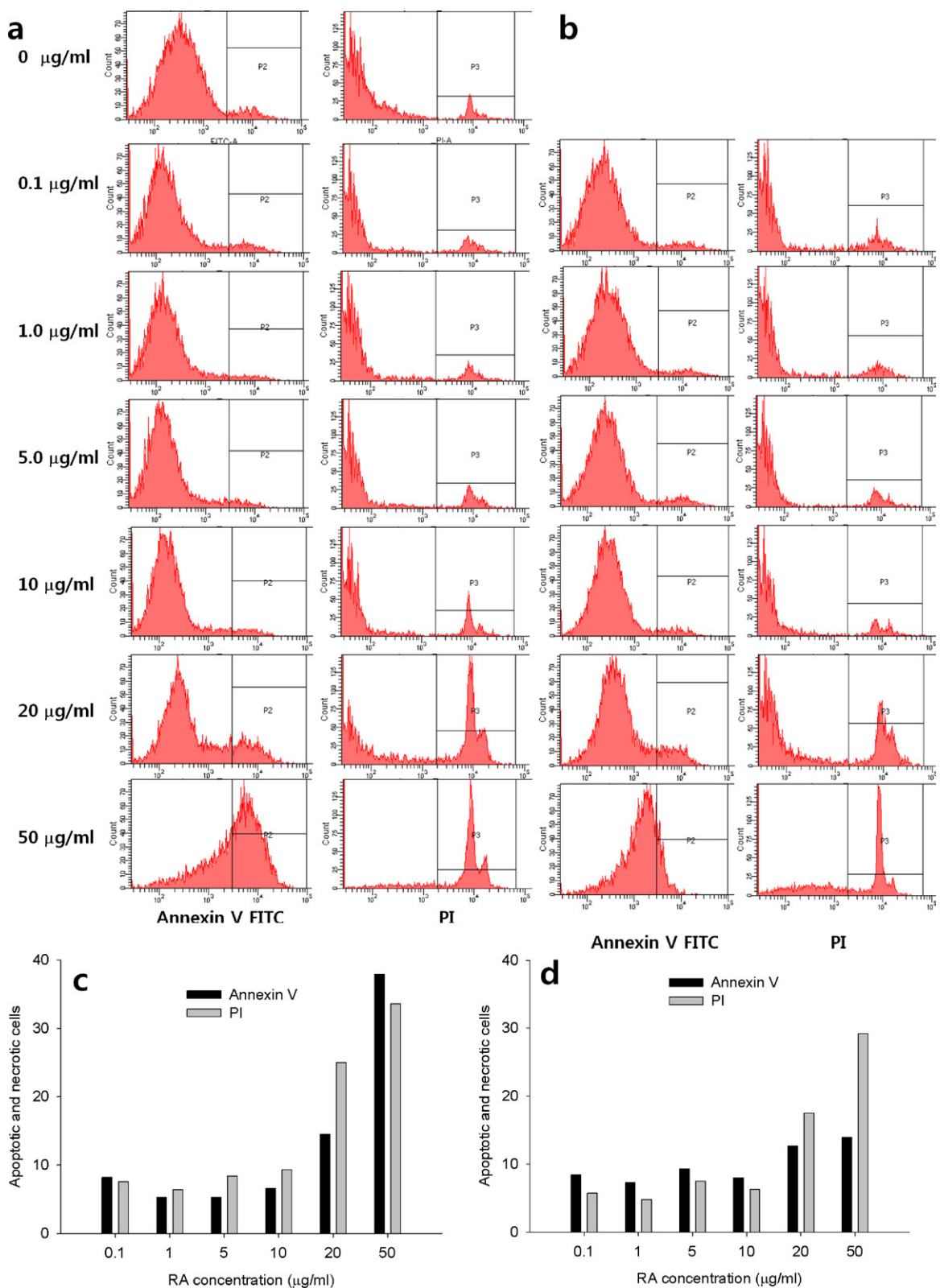


Fig. 4. Flow cytometry analysis of HuCC-T1 human CC cells. Annexin V were used for apoptosis analysis and PI were used for necrosis analysis. (a) and (c) RA alone; (b) and (d) RA-incorporated GC nanoparticles.

days, as shown in Fig. 3(a) and (b), while the number of surviving cells decreased in a dose dependent manner at day 3. As shown in Fig. 3(a), RA-incorporated GC nanoparticles demonstrated an inhibitory effect similar to that of RA alone. However, at days 2 (Fig. 3(b)) and 3 (Fig. 3(c)), the number of viable tumor cells was

decreased in a dose dependent manner and the RA-incorporated GC nanoparticles showed a slightly higher inhibitory effect against tumor cells at a concentration $<20 \mu\text{g/mL}$.

In a cell cytotoxicity assay, RA and RA-incorporated GC nanoparticles demonstrated dose-dependent toxic effects against HuCC-T1

cells, as shown in Fig. 3(d)–(f). The viability of tumor cells was decreased in a dose dependent manner until reaching a RA treatment concentration of 50 $\mu\text{g}/\text{mL}$, while the number of viable cells following treatment with RA-incorporated GC nanoparticles was not significantly decreased at a concentration $>10 \mu\text{g}/\text{mL}$.

Empty GC nanoparticles did not demonstrate any significant effect on the viability of tumor cells, as shown in Fig. 3(g) and (h). In the proliferation inhibition study (Fig. 3(g)), empty GC nanoparticles did not significantly inhibit the proliferation of tumor cells. Especially, proliferation of tumor cells was $>95\%$ at all GC concentration ranges at day 1 of treatment, even though the growth index of tumor cells was slightly decreased at day 2. In the cell cytotoxicity assay, empty GC nanoparticles did not significantly affect the viability of tumor cells; i.e., $>80\%$ of tumor cells survived at any concentration of GC and at any time course. These results indicated that GC itself did not affect the proliferation of tumor cells.

Fig. 4 shows analyses of apoptosis and necrosis of HuCC-T1 cells using Annexin V FITC and PI. As shown in Fig. 4(a), the numbers of apoptotic and necrotic cells were not significantly increased until reaching a of RA concentration of 10 $\mu\text{g}/\text{mL}$. At RA concentrations $>10 \mu\text{g}/\text{mL}$, the numbers of both apoptotic and necrotic cells were significantly increased in a dose-dependent manner. At RA concentrations $<20 \mu\text{g}/\text{mL}$, apoptosis was relatively dominant in the cell cytotoxicity behaviour of RA. Otherwise, necrosis was relatively dominant with nanoparticle treatment. These results indicated that the viability of tumor cells was gradually decreased at RA concentrations $>10 \mu\text{g}/\text{mL}$. Fig. 5 shows the invasive capacity of HuCC-T1 CC cells according to treatment with RA or RA-incorporated GC nanoparticles. As shown in Fig. 5(a), the number of cells which migrated through Matrigel® gradually decreased according to the increase of RA concentration for both RA and RA-incorporated nanoparticles. Especially, invasiveness of tumor cells was mostly inhibited at an RA concentration of 50 $\mu\text{g}/\text{mL}$. Even though the number of invasive cells was slightly higher than that with RA treatment at 50 $\mu\text{g}/\text{mL}$, RA-incorporated GC nanoparticles had at least an equal anti-invasive capacity compared to RA alone. Empty nanoparticles did not affect the invasiveness of tumor cells, as shown in Fig. 5(b). These results indicated that RA and RA-incorporated GC nanoparticles have anti-invasive activity against HuCC-T1 CC cells.

Fig. 6 shows migration of HuCC-T1 CC cells using a wound healing assay. As shown in Fig. 6(a), migration of tumor cells was inhibited by treatment with RA or RA-incorporated GC nanoparticles, while tumor cells migrated and filled the wounds at when treated with control and empty nanoparticles (0 $\mu\text{g}/\text{mL}$ of RA or NP in Fig. 6). The migration of tumor cells was not significantly inhibited at 1 or 5 $\mu\text{g}/\text{mL}$ RA concentrations when using either RA itself or RA-incorporated GC nanoparticles. However, migration of tumor cells was inhibited by treatment with RA-incorporated GC nanoparticles at 10 $\mu\text{g}/\text{mL}$. These results indicated that RA-incorporated nanoparticles were an effective treatment to inhibit migration of HuCC-T1 CC cells.

4. Discussion

Nanoparticles are believed to be a promising vehicle to target cancer cells (Bharali et al., 2009; Jain, 2005; Sinha et al., 2006). Nanoparticles based on chitosan have been extensively investigated for cancer chemotherapy and imaging (Jeong et al., 2006; Kim et al., 2010; Wang et al., 2011). Superior biocompatibility, lack of cytotoxicity, and biologically active properties (Kim et al., 2010; Wang et al., 2011) are frequently cited as advantages of chitosan as a biomedical material and drug carrier (Wang et al., 2011). Furthermore, chitosan is regarded as an ideal vehicle for tumor targeting and gene delivery because the amine group of chitosan can be used as a reactive group for chemical modification, drug conjugation and ion complex formation with anionic drugs (Jeong et al.,

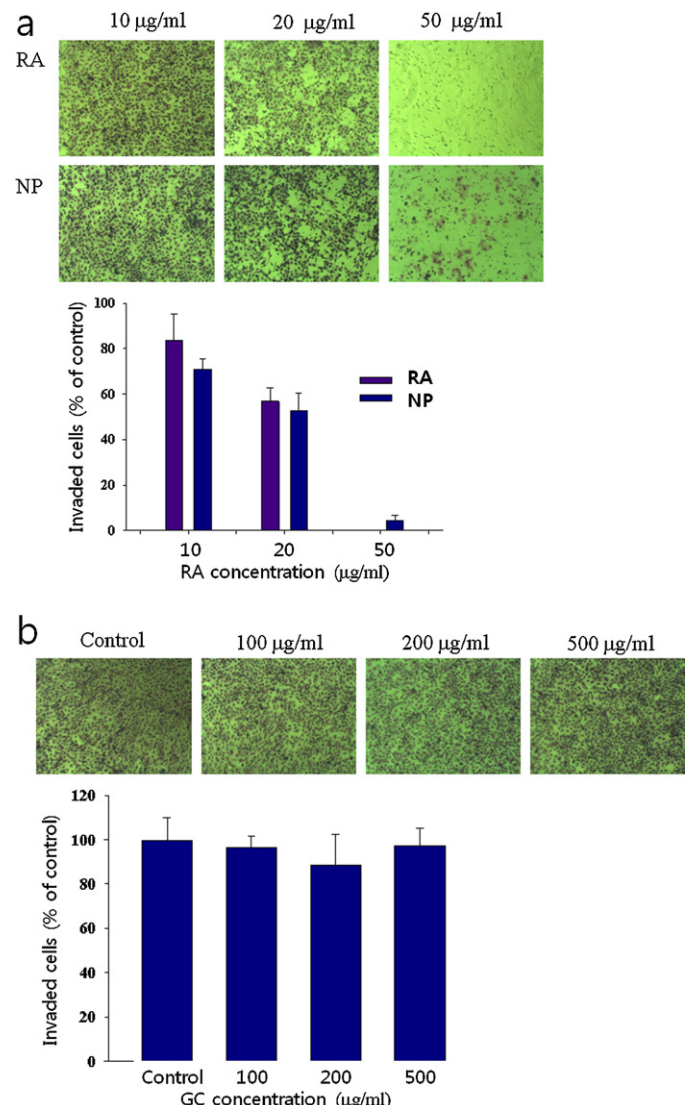


Fig. 5. The effect of RA or RA-incorporated GC nanoparticles on the invasiveness of HuCC-T1 human CC cells. Matrigel assay was used to test invasive capacity of tumor cells. (a) RA or RA-incorporated GC nanoparticles (NP); (b) empty GC nanoparticles.

2006; Kim et al., 2010; Wang et al., 2011; Yoo et al., 2005). Jeong et al. (2006) reported that methoxy poly(ethylene glycol)(PEG)-grafted chitosan was used to make polyion complex micelles. The principle idea of nanoparticle formation between RA and positively charged macromolecules was derived from reports by Thünemann and Beyermann (Thünemann and Beyermann, 2000; Thünemann et al., 2000). They prepared nanocomplexes using RA and polyethyleneimine or PEG-*b*-poly(L-lysine) copolymer. We prepared RA-incorporated GC nanoparticles by simple mixing of an RA organic solution with a GC aqueous solution, followed by removal of organic solvent by dialysis. Even though the particle size of RA-incorporated GC nanoparticles was larger than we expected, they had spherical shapes with a size $<500 \text{ nm}$. Especially, lyophilized nanoparticles were easily reconstituted into aqueous solution in spite of the absence of cryoprotectants. The size of reconstituted nanoparticles was not significantly changed (data not shown). In the absence of RA, GC itself did not form nanoparticles.

CC is a malignant tumor arising from the epithelium of the bile ducts (Lim, 2003). CC is normally classified into 3 groups; i.e., mass-forming, periductal-infiltrating, and intraductal-growing types (Lim, 2003). Intrinsic properties of cholangiocarcinoma are

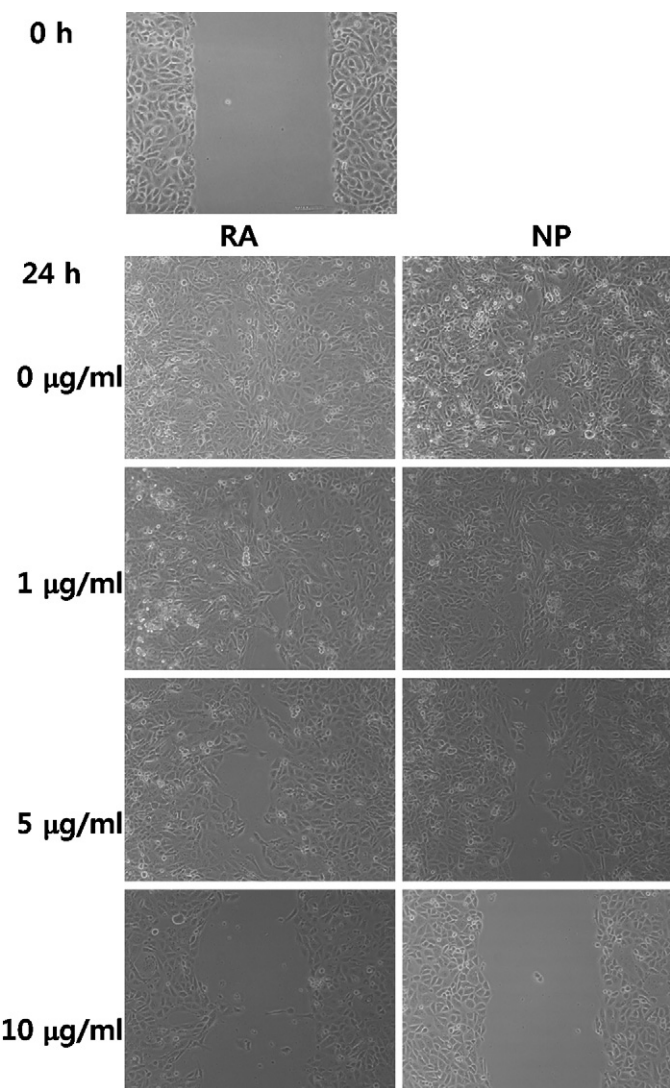


Fig. 6. The effect of RA or RA-incorporated GC nanoparticles on the migration of HuCC-T1 human CC cells.

broadly described as follows: (1) glandular structures growing in cellular nests; (2) tendency for spreading between the hepatocyte plates, along the duct walls, and adjacent to nerves; (3) perineural invasion (Bhuiya et al., 1992; Lim, 2003; Rosai, 1996). Especially, higher than 80% of reported case is known to have perineural invasion (Bhuiya et al., 1992; Lim, 2003). Perineural invasion in CC, which is a common path for CC metastasis, is highly correlated with postoperative recurrence and poor prognosis (Shen et al., 2010). Furthermore, it often appears early stage of tumor progression. Because of most CC patients cannot be effectively treated by surgery, a palliative therapeutic strategy is required to treat CC. Since CC is known to be resistant to traditional chemotherapeutic agents (Blechacz and Gores, 2008; Sirica, 2005), novel treatment option should be considered in the chemotherapy based on physiological properties of CC such as proliferation, invasion, metastasis, and spreading (Bhuiya et al., 1992; Rosai, 1996).

The aim of this study was to investigate the antitumor activity of nanoparticles incorporating RA *in vitro*. We selected RA as a chemotherapeutic agent because RA is known to inhibit proliferation, migration, and invasion of tumor cells (Bouterfa et al., 2000; Rotan, 1991). As shown in Fig. 3(a)–(c), RA and RA-incorporated GC nanoparticles were effective for inhibiting proliferation of HuCC-T1 CC cells. In the proliferation inhibition test, RA and RA-incorporated

GC nanoparticles at day 1 of treatment significantly inhibited proliferation at RA concentrations $>20 \mu\text{g}/\text{mL}$, and the growth of tumor cells was inhibited in a dose dependent manner at 3 days of treatment. The cytotoxicity study showed that the viability of tumor cells was decreased in a dose dependent manner until reaching an RA concentration of $20 \mu\text{g}/\text{mL}$, as shown in Fig. 3(d)–(f). Results from apoptosis and necrosis assays of HuCC-T1 CC cells are shown in Fig. 4, and correspond to the results in Fig. 3. As shown in Fig. 5, the invasion of tumor cells was gradually decreased according to the increase of RA concentration for both RA and RA-incorporated GC nanoparticles, while empty GC vehicles did not affect to the invasiveness of tumor cells. RA is known to have strong anti-invasive effect against tumor cells (Adachi et al., 2001; Papi et al., 2007; Rotan, 1991). Jeong et al. (2006) reported that RA or RA-incorporated nanoparticles have effectiveness in the inhibition of migration of malignant glioblastoma cells. Our results also showed that RA-incorporated GC nanoparticles inhibited the migration of tumor cells to a degree similar to RA itself (Fig. 6), while empty GC vehicles did not significantly affect the migration of tumor cells. Adachi et al. (2001) also reported that 3 types of RA (all-trans retinoic acid, 13-cis retinoic acid, and 9-cis retinoic acid) were effective for inhibiting invasion and migration of various human colon cancer cells *in vitro*. Papi et al. (2007) reported that invasion of the U87MG glioblastoma cell line and its related proteins were decreased by treatment with RA. Furthermore, Hashida group (Charoensit et al., 2010; Suzuki et al., 2006) demonstrated that RA-incorporated cationic liposomes were efficiently inhibited pulmonary metastasis of colon carcinoma cells. They also demonstrated that RA-incorporated cationic liposomes have inhibitory effect for the liver metastasis of colon carcinoma cells (Chansri et al., 2006).

In our results, although RA-incorporated GC nanoparticles were not superior to RA itself, they maintained the antitumor activity of RA and properly inhibited proliferation, invasion, and migration of HuCC-T1 CC cells.

5. Conclusion

We prepared RA-incorporated GC nanoparticles and their antitumor activity was studied using HuCC-T1 CC cells. RA-incorporated GC nanoparticles had spherical shapes and a narrow size distribution. RA-incorporated GC nanoparticles demonstrated similar anti-proliferative effects against HuCC-T1 CC cells when compared to RA alone, while empty GC vehicles did not affect the viability of tumor cells. Analysis of tumor cells for apoptosis and necrosis after treatment with RA or RA-incorporated GC nanoparticles also supported these results. An invasion test using Matrigel® also showed that invasion of tumor cells was significantly inhibited at RA concentrations $>20 \mu\text{g}/\text{mL}$. A wound healing assay also showed that RA-incorporated GC nanoparticles inhibited migration of tumor cells to a degree similar to RA itself. Our results suggested that RA-incorporated GC nanoparticles are promising vehicles for RA delivery to HuCC-T1 CC cells.

Acknowledgements

This study was supported by a grant of the Korean Healthcare Technology R&D Project, Ministry of Health and Welfare, Republic of Korea (Project No. A091047).

References

- Adachi, Y., Itoh, F., Yamamoto, H., Iku, S., Matsuno, K., Arimura, Y., Imai, K., 2001. Retinoic acids reduce matrix metalloproteinase 7 and inhibit tumor cell invasion in human colon cancer. *Tumour Biol.* 22, 247–253.
- Blechacz, B.R., Gores, G.J., 2008. Cholangiocarcinoma. *Clin. Liver Dis.* 12, 131–150.

Bharali, D.J., Khalil, M., Gurbuz, M., Simone, T.M., Mousa, S.A., 2009. Nanoparticles and cancer therapy: a concise review with emphasis on dendrimers. *Int. J. Nanomed.* 4, 1–7.

Bouterfa, H., Picht, T., Keb, D., Herbold, M.C.S.C., Noll, E., Black, P.M., Roosen, K., Tonn, J.C., 2000. Retinoids inhibit human glioma cell proliferation and migration in primary cell cultures but not in established cell lines. *Neurosurgery* 46, 419–430.

Bhuiya, M.R., Nimura, Y., Kamiya, J., Kondo, S., Hayakawa, N., Shionoya, S., 1992. Clinicopathologic studies on perineural invasion of bile duct carcinoma. *Ann. Surg.* 215, 344–349.

Chansri, N., Kawakami, S., Yamashita, F., Hashida, M., 2006. Inhibition of liver metastasis by all-trans retinoic acid incorporated into O/W emulsions in mice. *Int. J. Pharm.* 321, 42–49.

Charoensit, P., Kawakami, S., Higuchi, Y., Yamashita, F., Hashida, M., 2010. Enhanced growth inhibition of metastatic lung tumors by intravenous injection of ATRA-cationic liposome/IL-12 pDNA complexes in mice. *Cancer Gene Ther.* 17, 512–522.

Choi, Y., Kim, S.Y., Kim, S.H., Lee, K.S., Kim, C., Byun, Y., 2001. Long-term delivery of all-trans-retinoic acid using biodegradable PLLA/PEG-PLLA blended microspheres. *Int. J. Pharm.* 215, 67–81.

Conley, B.A., Egorin, M.J., Sridaha, R., Finley, R., Hemady, R., Wu, S., Tait, N.S., Van Echo, D.A., 1997. Phase I clinical trial of all-trans-retinoic acid with correlation of its pharmacokinetics and pharmacodynamics. *Cancer Chem. Pharm.* 39, 291–299.

Defer, G.L., Adle-Biassette, H., Ricolfi, F., Martin, L., Authier, F.J., Chomienne, C., Degos, L., Degos, J.D., 1997. All-trans retinoic acid in relapsing malignant gliomas: clinical and radiological stabilization associated with the appearance of intratumoral calcifications. *J. Neurooncol.* 34, 169–177.

Estey, E.H., Giles, F.J., Kantarjian, H., O'Brien, S., Cortes, J., Freireich, E.J., Lopez-Berestein, G., Keating, M., 1999. Molecular remissions induced by liposomal-encapsulated all-trans retinoic acid in newly diagnosed acute promyelocytic leukemia. *Clin. Observ. Interv. Ther.* 94, 2230–2235.

Frankel, S.R., Eardley, A., Lauwers, G., Weiss, M., Warrell, R.P., 1992. The “retinoic acid syndrome” in acute promyelocytic leukemia. *Ann. Intern. Med.* 117, 292–296.

Giannini, F., Maestro, R., Vukosa, T., Vljevic, T., Pomponi, F., Boiocchi, M., 1997. All-trans, 13-cis and 9-cis retinoic acids induce a fully reversible growth inhibition in HNSCC cell lines: implications for in vivo retinoic acid use. *Int. J. Cancer* 70, 194–200.

Giordano, G.G., Refojo, M.F., Arroyo, M.H., 1993. Sustained delivery of retinoic acid from microspheres of biodegradable polymer in PVR. *Invest. Ophtal. Vis. Sci.* 34, 2743–2751.

Huang, E.J., Ye, Y.C., Chen, S.R., Chai, J.R., Lu, J.X., Zhoa, L., Gu, L.J., Wang, Z.Y., 1988. Use of all-trans retinoic acid in the treatment of acute promyelocytic leukemia. *Blood* 72, 567–572.

Jain, K.K., 2005. Nanotechnology-based drug delivery for cancer. *Technol. Cancer Res. Treat.* 4, 407–416.

Jeong, Y.I., Kim, S.H., Jung, T.Y., Kim, I.Y., Kang, S.S., Jin, Y.H., Ryu, H.H., Sun, H.S., Jin, S.G., Kim, K.K., Ahn, K.Y., Jung, S., 2006. Polyion complex micelles composed of all-trans retinoic acid and poly(ethylene glycol)-grafted chitosan. *J. Pharm. Sci.* 95, 2348–2360.

Jin, S.G., Jeong, Y.I., Jung, S., Ryu, H.H., Jin, Y.H., Kim, I.Y., 2009. The effect of hyaluronic acid on the invasiveness of malignant glioma cells: comparison of invasion potential at hyaluronic acid hydrogel and matrigel. *J. Korean Neurosurg. Soc.* 46, 472–478.

Kalmekarian, G.P., Jasti, R.K., Celano, P., Nelkin, B.D., Marby, M., 1994. All-trans retinoic acid alters myc gene expression and inhibits in vitro progression in small-cell lung cancer. *Cell Growth Differ.* 5, 55–60.

Kim, C.H., Chung, C.W., Choi, K.H., Yoo, J.J., Kim, D.H., Jeong, Y.I., Kang, D.H., 2011. Effect of 5-aminolevulinic acid-based photodynamic therapy via reactive oxygen species in human cholangiocarcinoma cells. *Int. J. Nanomed.* 6, 1357–1363.

Kim, K., Kim, J.H., Park, H., Kim, Y.S., Park, K., Nam, H., Lee, S., Park, J.H., Park, R.W., Kim, I.S., Choi, K., Kim, S.Y., Park, K., Kwon, I.C., 2010. Tumor-homing multifunctional nanoparticles for cancer theragnosis: simultaneous diagnosis, drug delivery, and therapeutic monitoring. *J. Control Release* 146, 219–227.

Krupitza, G., Hull, W., Harant, H., Dittrich, E., Kallay, E., Huber, H., 1995. Retinoic acid induced death of ovarian carcinoma cells correlates with c-myc stimulation. *Int. J. Cancer* 61, 649–659.

Lehman, P.A., Slattery, J.T., Franz, T.J., 1988. Percutaneous absorption of retinoids: influence of vehicle, light exposure, and dose. *J. Invest. Dermatol.* 91, 56–61.

Lim, J.H., 2003. Cholangiocarcinoma: morphologic classification according to growth pattern and imaging findings. *AJR Am. J. Roentgenol.* 181, 819–827.

Lim, S.J., Kim, C.K., 2002. Formulation parameters determining the physicochemical characteristics of solid lipid nanoparticles loaded with all-trans retinoic acid. *Int. J. Pharm.* 243, 135–146.

Morris-Kay, G. (Ed.), 1992. *Retinoids in Normal Development and Teratogenesis*. Oxford Science Publications, Oxford.

Muindi, J.R.F., Frankel, S.R., Miller, W.H., Jakubowski, A., Scheinberg, D.A., Young, C.W., Dmitrovsky, E., Warrell, R.P., 1992. Continuous treatment with all-trans-retinoic acid causes a progressive reduction in plasma drug concentrations: implications for relapse and retinoid “resistance” in patients with acute promyelocytic leukemia. *Blood* 79, 299–303.

Noll, E., Miller, R.H., 1994. Regulation of oligodendrocyte differentiation: a role for retinoic acid in the spinal cord. *Development* 120, 649–660.

Papi, A., Bartolini, G., Ammar, K., Guerra, F., Ferreri, A.M., Rocchi, P., Orlandi, M., 2007. Inhibitory effects of retinoic acid and IIF on growth, migration and invasiveness in the U87MG human glioblastoma cell line. *Oncol. Rep.* 18, 1015–1021.

Reddy, S.B., Patel, T., 2006. Current approaches to the diagnosis and treatment of cholangiocarcinoma. *Curr. Gastroenterol. Rep.* 8, 30–37.

Rosai, J., 1996. *Ackerman's Surgical Pathology*, 8th ed. St. Louis, Mosby, pp. 914–915.

Rotan, R., 1991. Retinoids as modulators of tumor cell invasion and metastasis. *Semin. Cancer Biol.* 2, 197–208.

Sandhu, D.S., Roberts, L.R., 2008. Diagnosis and management of cholangiocarcinoma. *Curr. Gastroenterol. Rep.* 48, 43–52.

Shen, F.Z., Zhang, B.Y., Feng, Y.J., Jia, Z.X., An, B., Liu, C.C., Deng, X.Y., Kulkarni, A.D., Lu, Y., 2010. Current research in perineural invasion of cholangiocarcinoma. *J. Exp. Clin. Cancer Res.* 29, 24.

Sinha, R., Kim, G.J., Nie, S., Shin, D.M., 2006. Nanotechnology in cancer therapeutics: bioconjugated nanoparticles for drug delivery. *Mol. Cancer Ther.* 5, 1909–1917.

Singh, P., Patel, T., 2006. Advances in the diagnosis, evaluation and management of cholangiocarcinoma. *Curr. Opin. Gastroenterol.* 22, 294–299.

Sirica, A.E., 2005. Cholangiocarcinoma: molecular targeting strategies for chemoprevention and therapy. *Hepatology* 41, 5–15.

Suzuki, S., Kawakami, S., Chansri, N., Yamashita, F., Hashida, M., 2006. Inhibition of pulmonary metastasis in mice by all-trans retinoic acid incorporated in cationic liposomes. *J. Control Release* 116, 58–63.

Szuts, E.Z., Harosi, F.I., 1991. Solubility of retinoids in water. *Arch. Biochem. Biophys.* 287, 297–304.

Thünemann, A.F., Beyermann, J., 2000. Polyethyleneimine complexes with retinoic acid: structure, release profiles, and nanoparticles. *Macromolecules* 33, 6878–6885.

Thünemann, A.F., Beyermann, J., Kukula, H., 2000. Poly(ethylene oxide)-b-poly(L-lysine) complexes with retinoic acid. *Macromolecules* 33, 5906–5911.

Welzel, T.M., McGlynn, K.A., Hsing, A.W., O'Brien, T.R., Pfeiffer, R.M., 2006. Impact of classification of hilar cholangiocarcinomas (Klastskin tumors) on the incidence of intra- and extrahepatic Cholangiocarcinoma in the United States. *J. Natl. Cancer Inst.* 98, 873–875.

Wang, J.J., Zeng, Z.W., Xiao, R.Z., Xie, T., Zhou, G.L., Zhan, X.R., Wang, S.L., 2011. Recent advances of chitosan nanoparticles as drug carriers. *Int. J. Nanomed.* 6, 765–774.

Yoo, H.S., Lee, J.E., Chung, H., Kwon, I.C., Jeong, S.Y., 2005. Self-assembled nanoparticles containing hydrophobically modified glycol chitosan for gene delivery. *J. Control Release* 103, 235–243.